Protoplasma (2009) 236:107–112
DOI 10.1007/s00709-009-0056-5

SHORT COMMUNICATION

Transient gene suppression in a red alga, *Cyanidioschyzon merolae* 10D

Mio Ohnuma · Osami Misumi · Takayuki Fujiwara · Satoru Watanabe · Kan Tanaka · Tsuneyoshi Kuroiwa

Received: 11 March 2009 / Accepted: 27 May 2009 / Published online: 17 June 2009

Abstract Antisense suppression is a powerful tool to analyze gene function. In this study, we show that antisense RNA suppressed the expression of a target gene in the unicellular red alga, *Cyanidioschyzon merolae*. In this study, the antisense strand of the *catalase* gene was cloned and inserted into an expression vector upstream of the *GFP* gene. This plasmid was introduced into *C. merolae* cells using a polyethylene glycol-mediated transformation protocol. Using the expression of GFP as a marker of transformed cells, the expression of catalase was examined by immunocytochemistry. Decreased expression of catalase was observed in cells that were transformed with the antisense strand of the *catalase* gene. These results indicate the utility of this antisense suppression system.

Keywords Antisense suppression · *Cyanidioschyzon merolae* · Catalase · GFP · Transformation

Abbreviations
DAPI 4′,6-diamidino-2-phenylindole
PEG polyethylene glycol

M. Ohnuma (✉) · O. Misumi · T. Fujiwara · T. Kuroiwa
Research Information Center for Extremophile,
Rikkyo University,
3-34-1 Nishiikebukuro,
Toshima-ku, Tokyo 171-8501, Japan
e-mail: mioohnuma@rikkyo.ac.jp

S. Watanabe · K. Tanaka
Institute of Molecular and Cellular Biosciences,
The University of Tokyo,
1-1-1 Yayoi,
Bunkyo-ku, Tokyo 113-0032, Japan

K. Tanaka
Graduate School of Horticulture, Chiba University,
648 Matsudo,
Matsudo, Chiba 271-8510, Japan

Introduction

Cyanidioschyzon merolae 10D is a unicellular red alga that lives in sulfate-rich, acid hot springs. *C. merolae* has one nucleus, one mitochondrion, and one plastid. *C. merolae* also contains of a minimum set of single membrane-bound organelles: one microbody (peroxisome), one Golgi apparatus, one endoplasmic reticulum, and a small number of lysosomes (Kuroiwa et al. 1994). In addition, the cell cycle phase of *C. merolae* can be easily synchronized by light and dark cycles (Suzuki et al. 1994). These characteristics have facilitated extensive biochemical and cell biological studies, especially on chloroplast and mitochondrial division and on mitotic partitioning of the microbody and vacuole (Miyagishima et al. 1999; Nishida et al. 2005, 2007; Yagisawa et al. 2007; Yoshida et al. 2006).

The complete sequences of the nuclear, mitochondrial, and plastid genomes of *C. merolae* have been determined (Matsuzaki et al. 2004; Nozaki et al. 2007; Ohta et al. 1998, 2003). Genomic analyses have revealed that *C. merolae* has the simplest genome, with the smallest redundancy, of any photosynthetic eukaryote so far analyzed. For example, there are only three ribosomal RNA gene clusters, the smallest known histone gene cluster, and very few introns and transposable elements (Matsuzaki et al. 2004; Nozaki et al. 2007). Phylogenetic analyses also support *C. merolae* as having diverged very early in the eukaryotic lineage (Nozaki et al. 2003) and primitive characteristics appear to have been conserved throughout evolution. These features indicate that *C. merolae* is an excellent model organism to study the function of genes.

C. merolae is an attractive organism for molecular genetic studies because its nuclear genome sequence has been determined (Matsuzaki et al. 2004; Nozaki et al. 2007). However, studies have been hindered by an inability

to introduce exogenous DNA into *C. merolae* cells. Recently, we developed a DNA transformation technique and performed transient expression of an exogenous gene in *C. merolae* (Ohnuma et al. 2008). To analyze gene function, disruption of the target gene is useful. However, gene knockout by homologous recombination of *C. merolae* is time consuming, and it cannot be employed for essential genes. Using our transient expression technique, we attempted the establishment of transient antisense suppression, which is a powerful method to downregulate gene expression (Schroda 2006). In this study, we introduced DNA containing the antisense strand of the *catalase* gene and successfully observed a decrease of catalase expression. These results are the first example of antisense suppression in *C. merolae* and indicate the utility of this antisense suppression system.

Materials and methods

Culture

C. merolae 10D was used in this study. Cells were grown in MA2 medium (Ohnuma et al. 2008) in a glass vessel under continuous white light (100 μmol photon m^{-2} s^{-1}) at 40°C.

Plasmid construction

The 35S promoter of Cauliflower mosaic virus (CaMV35S promoter) exists upstream of *sGFP* in pTH-2 (Niwa 2003). pTH-2 was digested with *Bam*HI and then self-ligated to remove the CaMV35S promoter to make pTH-2PL.

Using the oligonucleotide primers, cat_PromF1_XbaI (5′-agctagTCTAGAagcagatagttcatagagttaggaggg-3′) and cat_PromR1500_BamHI (5′-cgccgcGGATCCcactaatatt gaaaacttcagcccagaatc-3′; the recognition sites of restriction enzymes are capitalized) and *C. merolae* DNA as a template, polymerase chain reaction (PCR) was carried out for 30 cycles (98°C for 10 s, 55°C for 5 s, and 68°C for 3 min) with PrimeSTAR® HS DNA Polymerase (TaKaRa Bio, Otsu, Japan). The amplified fragment was digested with *Xba*I and *Bam*HI and substituted for the *Xba*I–*Bam*HI fragment of pTH-2PL to make pI050P-GFP. pI050P-GFP has the 5′-flanking region of the *catalase* gene (1,500 bp) instead of the CaMV35S promoter.

The 5′-flanking region and open reading frame (ORF) of the *catalase* gene (2,988 bp) was amplified using of the oligonucleotide primers, cat_PromF1_XbaI and cat_GeneR2988_BamHI (5′-cgccgcGGATCCcattgtacactgcttc actctggt-3′). PCR was carried out as described above. The amplified fragment was digested with *Xba*I and *Bam*HI and substituted for the *Xba*I–*Bam*HI fragment of pTH-2PLto make pI050S-GFP. pI050S-GFP has a 1,500-bp 5′-flanking region of the *catalase* gene and a 1,488-bp *catalase* ORF fused to *sGFP*.

To obtain the antisense strand of the *catalase* ORF adjacent to the 5′-flanking region, the 5′-flanking region and the antisense strand of the *catalase* ORF were amplified individually. Using the oligonucleotide primers, cat_PromF1_XbaI (5′-agctagTCTAGAagcagatagttcatagagt taggaggg-3′) and I050ASprom-R (5′-*gagtgaagcagtgta caatg*cactaatattgaaaact-3′; italicized sequence indicates *catalase* ORF antisense sequence) and *C. merolae* DNA as a template, the 5′-flanking region (1,500 bp) was amplified. PCR was carried out for 30 cycles (98°C for 10 s, 55°C for 5 s, and 68°C for 2 min) with PrimeSTAR® HS DNA Polymerase (TaKaRa Bio, Otsu, Japan). Similarly, the antisense strand of the *catalase* ORF (1,488 bp) was amplified using the oligonucleotide primers, I050AS-F (5′-agttttcaatattagtg*cattgtacactgcttcactc*-3′) and I050AS-R (5′-cgccgcGGATCC*atggacccaaccaagtatac*-3′). Amplified fragments of the *catalase* 5′-flanking region and the antisense strand of the *catalase* ORF were separated by electrophoresis and purified using the QIAquick gel extraction kit (Qiagen, Hilden, Germany). PCR (98°C for 10 s, 60°C for 5 s, and 68°C for 3 min) was performed with these fragments without template for ten cycles to make a fused DNA fragment (2,988 bp). Then, using the fused fragment as a template, PCR was carried out with primers cat_PromF1_XbaI and I050AS-R for 20 cycles (98°C for 10 s, 55°C for 5 s, and 68°C for 3 min) to amplify a DNA fragment of the antisense strand of the *catalase* ORF adjacent to the 5′-flanking region. The amplified fragment was digested with *Xba*I and *Bam*HI and substituted for the *Xba*I–*Bam*HI fragment of pTH-2PL to make pI050AS-GFP. pI050AS-GFP has a 1,500-bp 5′-flanking region of the *catalase* gene and a 1,488-bp antisense fragment of the *catalase* ORF adjacent to *sGFP*.

Antibody generation

To generate a rat catalase antiserum, a full-length bacterial recombinant protein (496 aa) of CMI050C with a six-histidine N-terminal tag was used for immunization.

Transformation

Transformation of *C. merolae* was performed as described previously (Ohnuma et al. 2008). Transformation efficiency was calculated as the percentage of GFP-positive cells in the total number of polyethylene glycol (PEG)-treated cells. Transformation was performed in triplicate and immunostained cells from three independent visual fields were counted for each sample. At least 2,000 cells were counted for each plasmid.

Immunocytochemistry

Cell fixation and immunocytochemistry were performed as described previously (Ohnuma et al. 2008). The anticatalase antibody was used at a dilution of 1/1,000. The anti-GFP antibody (monoclonal antibody JL-8; Clontech, Mountain View, CA, USA) was used at a dilution of 1/200. Goat antirat IgG conjugated with Alexa 488 and highly cross-adsorbed goat antimouse IgG conjugated with Alexa 555 (Molecular Probes, Eugene, OR, USA) were used as the secondary antibodies at dilutions of 1/1,000. 4′,6-Diamidino-2-phenylindole (DAPI) staining was performed as previously described (Yagisawa et al. 2007). Images were captured as described previously (Nishida et al. 2005). The intensity of catalase signal was quantified as described (Kobayashi et al. 2009).

Results and discussion

We recently established a PEG-mediated transformation protocol for *C. merolae* (Ohnuma et al. 2008). In the present study, we tried to transiently suppress a target gene using this protocol. PEG-treated cells transform at low efficiency; therefore, a phenotype distinguishable by microscopy was required to examine antisense suppression within individual cells, rather than in the overall population. We, therefore, used *sGFP* to successfully distinguish transformed cells and we observed the behavior of microbodies to evaluate suppression. *C. merolae* has only one microbody and the microbody has a characteristic pattern of movement during cell cycle progression (Miyagishima et al. 1999; Misumi et al. 2005). At interphase, the microbody is located about midway between the nucleus and the mitochondrion in the lateral area of the cell. At prophase, the microbody associates with the dividing V-shaped mitochondrion. Around the time of completion of plastid and mitochondrial divisions (metaphase), microbody division starts. The *catalase* gene (CMI050C) was chosen as a target gene because it is a microbody marker and because the EST of *catalase* showed a high level of expression (http://merolae.biol.s.u-tokyo.ac.jp/db/estmap.cgi?locus=CMI050C). Since the core RNAi machinery components seem to be absent from *C. merolae* (Casas-Mollano et al. 2008), a full-length *catalase* antisense strand was used instead of an inverted repeat-containing construct. *sGFP* was added downstream of the *catalase* gene as a marker of transformation (Fig. 1a). Twenty-four hours after transformation, GFP fluorescence was observed directly in the cells (Fig. 1b). GFP fluorescence was strong in the cells that were transformed with pI050S-GFP, while that detected in the cells that were transformed with pI050P-GFP and pI050AS-GFP was extremely weak. GFP encoded on pI050S-GFP is a fusion protein, while the GFPs encoded on pI050P-GFP and pI050AS-GFP are not fusion proteins. GFP is possibly more susceptible to degradation than the GFP fusion, although the reason for this is unknown. Immunostaining of GFP made it easier to detect cells that were successfully transformed. Immunostained cells were counted to calculate the transformation efficiency (Fig. 1b). Transformation efficiency of pI050P-GFP and pI050AS-GFP was about threefold to fivefold lower compared with that of pI050S-GFP. This may result from the instability of GFP encoded on pI050P-GFP and pI050AS-GFP, which would result in an apparently lower transformation efficiency compared with that of pI050S-GFP. The cells were fixed 24 h after transformation and stained with anti-GFP and anticatalase antibodies and then analyzed by microscopy. First, we detected GFP-positive cells and then we observed catalase localization to evaluate the suppression of the *catalase* gene.

Localization of catalase in GFP-negative cells was examined by immunocytochemistry (Fig. 1c). These cells were PEG-treated, but were not transformed. At interphase, catalase was located about midway between the nucleus and the mitochondrion. At prophase, catalase associated with the dividing V-shaped mitochondrion. At metaphase, when the plastid and mitochondrial division is completed, two signals of catalase were observed. The behavior of catalase in nontransformed PEG-treated cells was the same as that of microbodies during normal cell cycle progression (Miyagishima et al. 1999; Misumi et al. 2005).

Detection of GFP by immunocytochemistry enabled the identification of cells successfully transformed with pI050P-GFP, pI050S-GFP, or pI050AS-GFP (Fig. 1d). To evaluate the effect of the antisense construct, localization and intensity of catalase signal was determined (Fig. 1e). We the quantified signal intensity per unit area of cytosol or of microbody using cells that were transformed with pI050AS-GFP. GFP-negative cells, PEG-treated but not transformed, showed intense signal at the microbody (GFP−; Fig. 1c, e). The pattern of localization and the intensity of catalase signal was varied in cells that were successfully transformed (GFP+). The pattern was classified into four groups. “Microbody” are cells that showed intense signal at the microbody. “Cytosol” are cells that showed dispersed signal in the cytosol. “Cytosol + microbody” are cells that showed both dispersed signal in the cytosol and pointed signal at the microbody. “Downregulated” are cells that showed no or weak signal at the microbody. There was no significant difference of localization and intensity of the signal between interphase and mitotic phase in each group.

The transformed cells were classified into these groups and the occurrence was analyzed. When cells were transformed with pI050P-GFP, *sGFP* was expressed from the *catalase* promoter and signal was located in the cytosol.

The catalase was localized to the microbody, regardless of the cell cycle phase (Fig. 1d [a], f). When cells were transformed with pI050S-GFP, the localization of catalase was varied in cells at interphase (Fig. 1d [b], f). However, catalase was localized to the microbody in most cells during the mitotic phase (Fig. 1d [c], f). When cells were transformed with pI050AS-GFP (Fig. 1d [d, e]), GFP signal was detected in the cytosol, indicating that *sGFP* was expressed from the *catalase* promoter even though there was 1.5 kb of *catalase* antisense strand upstream of *sGFP*. The intrinsic catalase signal was dramatically decreased and poorly localized to microbodies. The suppression was more efficiently observed in cells during the mitotic phase than at interphase (Fig. 1f). The antisense strand of the *catalase* gene successfully suppressed catalase expression in *C. merolae* during the mitotic phase.

Catalase was localized to the cytosol or to the cytosol and microbody in cells at interphase when pI050S-GFP or pI050AS-GFP was introduced into the cells (Fig. 1f). When cells were transformed with pI050AS-GFP, localization of catalase to the cytosol and microbody was also observed during the mitotic phase. The cytosolic localization of catalase in pI050S-GFP-transformed cells results from mistargeting due to overexpression, but the reason for mistargeting in pI050AS-GFP-transformed cells was unclear. Some cells transformed with the antisense construct, pI050AS-GFP, showed cytosolic localization of catalase; however, catalase was not significantly downregulated in cells that were transformed with pI050P-GFP and pI050S-GFP. Therefore, catalase was specifically downregulated by the antisense strand of catalase encoded on pI050AS-GFP.

C. merolae is an ideal model for the study of basic cellular functions for a number of reasons. First, *C. merolae* is a free-living, autotrophic organism and, therefore, it retains primitive but essential cell functions, despite having the smallest known genome of a photosynthetic eukaryote. Second, *C. merolae* has a simple cell structure, containing one nucleus, one mitochondrion, one plastid, and a minimal set of single membrane-bound organelles. Also, the sequences of the nuclear, mitochondrial, and plastid genomes are available (Matsuzaki et al. 2004; Nozaki et al. 2007; Ohta et al. 1998, 2003) and the cell cycle phase of *C. merolae* can be completely synchronized by light treatment (Suzuki et al. 1994).

Biochemical and cell biological studies have been extensively preformed using this alga; however, the development of genetic techniques was required to make *C. merolae* experimentally tractable. We previously established a method for DNA transformation, which is an essential technique for molecular genetics analyses (Ohnuma et al. 2008). In the present study, we attempted the knockdown of the target gene *catalase*. The antisense construct of *catalase* showed a suppression effect, thus this method enabled reverse genetics in *C. merolae*. Suppression of catalase is the first example of antisense suppression in *C. merolae*. We have also applied this method to studies on mitochondrial division and on the partition of lysosomes, which accompanies cell division. Downregulation of target genes associated with these functions resulted in aberrant division of the cell. These studies have been submitted for publication.

We are currently attempting to improve the efficiency of gene suppression. To improve transformation efficiency, we are optimizing plasmid and cell concentrations, the length time of PEG treatment, and the effects of carrier DNA. Our results suggested that *sGFP* is a useful indicator of cell transformation in this transient assay. However, as shown in Fig. 1b, *sGFP* encoded on pI050P-GFP and pI050AS-GFP was unstable. Using pI050S-GFP as a host plasmid to generate antisense constructs of genes of interest would be advantageous because fused *sGFP* fusion proteins are stable throughout the cell cycle. Depending on the target gene, GFP that localized to chloroplasts or mitochondria would allow easier observation. GFP fused to a chloroplast- or mitochondrion-targeted protein would be useful for this purpose. The HA tag on proteins would also be a useful

Fig. 1 **a** Plasmids used in this study. *Black line* represents the promoter region of *catalase*. *Filled arrow* represents the sense or antisense strand of *catalase*. *Open arrow* represents *sGFP*. **b** Direct observation of GFP. Cells are transformed with pI050P-GFP (*a*, *d*, *g*, *j*), pI050S-GFP (*b*, *e*, *h*, *k*), or pI050AS-GFP (*c*, *f*, *i*, *l*) are shown. Transformation efficiency of each plasmid is indicated in *parentheses*. Phase contrast (*PC*; *a–c*), GFP (*GFP*; *d–f*), intrinsic chlorophyll fluorescence (*Cp*; *g–i*), and merged images (*j–l*) are shown. Scale bars correspond to 1 μm. **c** Subcellular localization of catalase after transformation. pI050AS-GFP was introduced into cells but those not successfully transformed are shown as a control. Cells at interphase (*Int*; *a*, *d*, *g*, *j*, *m*, *p*), prophase (*Pro*; *b*, *e*, *h*, *k*, *n*, *q*), and metaphase (*Met*; *c*, *f*, *i*, *l*, *o*, *r*) are shown. Phase contrast (*PC*; *a–c*), catalase (*green*; *d–f*), GFP (*orange*; *g–i*), intrinsic chlorophyll fluorescence (*red*; *j–l*), DAPI-stained DNA (*blue*; *m–o*), and merged images (*p–r*) are shown. DAPI stained nuclear DNA (*n*), mitochondrial DNA (*mt*), chloroplast (*cp*), and microbody (*mi*) are indicated in the merged image (*p*). Scale bars correspond to 1 μm. **d** Subcellular localization of catalase in cells that were successfully transformed with pI050P-GFP (*a*; the *upper row*), pI050S-GFP (*b*, *c*; the *middle two rows*), and pI050AS-GFP (*d*, *e*; the *lower two rows*). Scale bars correspond to 1 μm. **e** Classification by localization and intensity of catalase signal. Signal intensity per unit area of cytosol (*open bar*) and of the microbody (*filled bar*) was analyzed in the cells that were transformed with pI050AS-GFP. The pattern of localization and intensity of the catalase signal were classified into four groups: "Microbody," "Cytosol," "Cytosol + Microbody," and "Downregulated." This classification is described in detail in the "Results and discussion" section. Unsuccessfully transformed cells and successfully transformed cells are indicated by GFP− and GFP+, respectively. The number of cells counted is indicated in *parentheses*. **f** Suppression efficiency of transformed cells at interphase or during mitotic phase. Localization of catalase in cells that were successfully transformed with pI050P-GFP (*open bar*), pI050S-GFP (*gray bar*), and pI050AS-GFP (*filled bar*) was analyzed. The cells were classified according to **e**. The cells at interphase (*Int*) or mitotic phase (*Mit*) were counted separately and the number of counted cells is indicated in *parentheses*. The number of cells counted was set as 100%

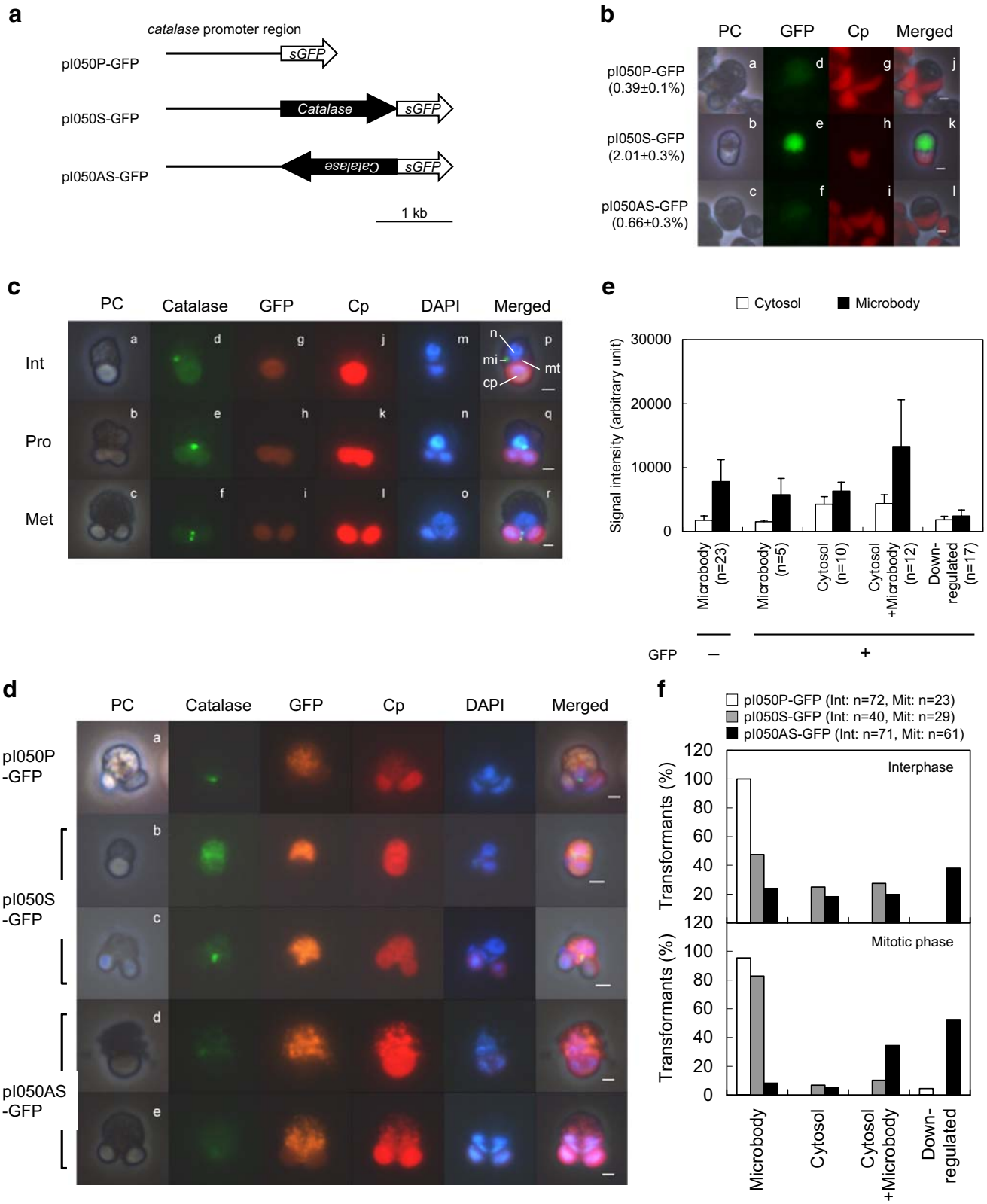
a
catalase promoter region
pI050P-GFP
sGFP
pI050S-GFP
Catalase
sGFP
pI050AS-GFP
Catalase
sGFP
1 kb
b
PC
GFP
Cp
Merged
pI050P-GFP (0.39±0.1%)
pI050S-GFP (2.01±0.3%)
pI050AS-GFP (0.66±0.3%)
c
PC
Catalase
GFP
Cp
DAPI
Merged
Int
Pro
Met
n
mi
cp
mt
e
Cytosol
Microbody
Signal intensity (arbitrary unit)
30000
20000
10000
0
Microbody (n=23)
Microbody (n=5)
Cytosol (n=10)
Cytosol +Microbody (n=12)
Down-regulated (n=17)
GFP
–
+
d
PC
Catalase
GFP
Cp
DAPI
Merged
pI050P -GFP
pI050S -GFP
pI050AS -GFP
f
pI050P-GFP (Int: n=72, Mit: n=23)
pI050S-GFP (Int: n=40, Mit: n=29)
pI050AS-GFP (Int: n=71, Mit: n=61)
Interphase
Mitotic phase
Transformants (%)
120
100
80
60
40
20
0
Microbody
Cytosol
Cytosol +Microbody
Down-regulated

marker in this system, as previously described (Ohnuma et al. 2008). The promoter of the *catalase* gene is constitutive. This is advantageous for the promoter driving GFP expression because GFP would be constitutively generated, making the identification of transformed cells easier. The native promoter of a target gene, instead of the catalase promoter, would be favorable to drive the expression of the antisense strand because it would be controlled in the same way as that of the target gene. Alternatively, when the expression of a target gene is phase-specific or conditional, a promoter that expresses strongly under the same conditions might be favorable. The effects of the region and length of the antisense strand on suppression efficiency also needs to be examined.

The percentage of transformants showing downregulation was 40–50% (Fig. 1f). In *Chlamydomonas*, percentage of transformants showing downregulation using an antisense construct varied between 0.3% and 50% (Schroda 2006). The major shortcoming of our system is the low transformation efficiency. In addition, plasmids used in this study lacked a selection marker for *C. merolae*. When a nonessential gene is the target, the effect of the antisense strand might last longer if the plasmid is maintained in the cell. This would allow for a more detailed examination of the target gene. Construction of a plasmid that can be maintained in *C. merolae* is in progress. Improvement of transformation efficiency and using a plasmid that is maintained in *C. merolae* cells would make not only cell biological studies but also biochemical studies possible.

Acknowledgments We thank Dr. Fumi Yagisawa for the technical assistance. This work was supported by the Frontier Project "Adaptation and Evolution of Extremophiles" from the Ministry of Education, Culture, Sports, Science and Technology of Japan and by the Program for the Promotion of Basic Research Activities for Innovative Biosciences (PROBRAIN) awarded to T.K. and by Grant-in-Aid for Creative Scientific Research (16GS0304) awarded to K.T.

Conflicts of interest The authors declare that they have no conflicts of interest.

References

Casas-Mollano JA, Rohr J, Kim EJ, Balassa E, van Dijk K, Cerutti H (2008) Diversification of the core RNA interference machinery in *Chlamydomonas reinhardtii* and the role of DCL1 in transposon silencing. Genetics 179:69–81. doi:10.1534/genetics.107.086546

Kuroiwa T, Kawazu T, Takahashi H, Suzuki K, Ohta N, Kuroiwa H (1994) Comparison of ultrastructures between the ultrasmall eukaryote *Cyanidioschyzon merolae* and *Cyanidium caldarium*. Cytologia (Tokyo) 59:149–158

Kobayashi Y, Kanesaki Y, Tanaka A, Kuroiwa H, Kuroiwa T, Tanaka K (2009) Tetrapyrrole signal as a cell-cycle coordinator from organelle to nuclear DNA replication in plant cells. Proc Natl Acad Sci U S A 106:803–807. doi:10.1073/pnas.0804270105

Matsuzaki M, Misumi O, Shin-i T, Maruyama S, Takahara M, Miyagishima S, Mori T, Nishida K, Yagisawa F, Nishida K, Yoshida Y, Nishimura Y, Nakao S, Kobayashi T, Momoyama Y, Higashiyama T, Minoda A, Sano M, Nomoto H, Oishi K, Hayashi H, Ohta F, Nishizaka S, Haga S, Miura S, Morishita T, Kabeya Y, Terasawa K, Suzuki Y, Ishii Y, Asakawa S, Takano H, Ohta N, Kuroiwa H, Tanaka K, Shimizu N, Sugano S, Sato N, Nozaki H, Ogasawara N, Kohara Y, Kuroiwa T (2004) Genome sequence of the ultrasmall unicellular red alga *Cyanidioschyzon merolae* 10D. Nature 428:653–657. doi:10.1038/nature02398

Misumi O, Matsuzaki M, Nozaki H, Miyagishima S, Mori T, Nishida K, Yagisawa F, Yoshida Y, Kuroiwa H, Kuroiwa T (2005) *Cyanidioschyzon merolae* genome. A tool for facilitating comparable studies on organelle biogenesis in photosynthetic eukaryotes. Plant Physiol 137:567–585. doi:10.1104/pp.104.053991

Miyagishima S, Itoh R, Toda K, Kuroiwa H, Nishimura M, Kuroiwa T (1999) Microbody proliferation and segregation cycle in the single-microbody alga *Cyanidioschyzon merolae*. Planta 208:326–336. doi:10.1007/s004250050566

Nishida K, Yagisawa F, Kuroiwa H, Nagata T, Kuroiwa T (2005) Cell cycle-regulated, microtubule-independent organelle division in *Cyanidioschyzon merolae*. Mol Biol Cell 16:2493–2502. doi:10.1091/mbc.E05-01-0068

Nishida K, Yagisawa F, Kuroiwa H, Yoshida Y, Kuroiwa T (2007) WD40 protein Mda1 is purified with Dnm1 and forms a dividing ring for mitochondria before Dnm1 in *Cyanidioschyzon merolae*. Proc Natl Acad Sci U S A 104:4736–4741. doi:10.1073/pnas.0609364104

Niwa Y (2003) A synthetic green fluorescent protein gene for plant biotechnology. Plant Biotechnol 20:1–11

Nozaki H, Matsuzaki M, Takahara M, Misumi O, Kuroiwa H, Hasegawa H, Shin-I T, Kohara Y, Ogasawara N, Kuroiwa T (2003) The phylogenetic position of red algae revealed by multiple nuclear genes from mitochondria-containing eukaryotes and an alternative hypothesis on the origin of plastids. J Mol Evol 56:485–497. doi:10.1007/s00239-002-2419-9

Nozaki H, Takano H, Misumi O, Terasawa K, Matuzaki M, Maruyama S, Nishida K, Yagisawa F, Yoshida Y, Fujiwara T, Takio S, Tamura K, Chung SJ, Nakamura S, Kuroiwa H, Tanaka K, Sato N, Kuroiwa T (2007) A 100%-complete sequence reveals unusually simple genomic features in the hot-spring red alga *Cyanidioschyzon merolae*. BMC Biol 5:28. doi:10.1186/1741-7007-5-28

Ohnuma M, Yokoyama T, Inouye T, Sekine Y, Tanaka K (2008) Polyethylene glycol (PEG)-mediated transient gene expression in a red alga, *Cyanidioschyzon merolae* 10D. Plant Cell Physiol 49:117–120. doi:10.1093/pcp/pcm157

Ohta N, Sato N, Kuroiwa T (1998) Structure and organization of the mitochondrial genome of the unicellular red alga *Cyanidioschyzon merolae* deduced from the complete nucleotide sequence. Nucleic Acids Res 26:5190–5198. doi:10.1093/nar/26.22.5190

Ohta N, Matsuzaki M, Misumi O, Miyagishima S, Nozaki H, Tanaka K, Shin-I T, Kohara Y, Kuroiwa T (2003) Complete sequence and analysis of the plastid genome of the unicellular red alga *Cyanidioschyzon merolae*. DNA Res 10:67–77. doi:10.1093/dnares/10.2.67

Schroda M (2006) RNA silencing in *Chlamydomonas*: mechanisms and tools. Curr Genet 49:69–84. doi:10.1007/s00294-005-0042-1

Suzuki K, Ehara T, Osafune T, Kuroiwa H, Kawano S, Kuroiwa T (1994) Behavior of mitochondria, chloroplasts and their nuclei during the mitotic cycle in the ultramicroalga *Cyanidioschyzon merolae*. Eur J Cell Biol 63:280–288

Yagisawa F, Nishida K, Kuroiwa H, Nagata T, Kuroiwa T (2007) Identification and mitotic partitioning strategies of vacuoles in the unicellular red alga *Cyanidioschyzon merolae*. Planta 226:1017–1029. doi:10.1007/s00425-007-0550-y

Yoshida Y, Kuroiwa H, Misumi O, Nishida K, Yagisawa F, Fujiwara T, Nanamiya H, Kawamura F, Kuroiwa T (2006) Isolated chloroplast division machinery can actively constrict after stretching. Science 313:1435–1438. doi:10.1126/science.1129689